

# MotionGen: Interactive Design and Editing of Planar Four-Bar Motions for Generating Pose and Geometric Constraints

Anurag Purwar<sup>1</sup>

Computer-Aided Design and Innovation Lab,  
Department of Mechanical Engineering,  
Stony Brook University,  
Stony Brook, NY 11794-2300  
e-mail: anurag.purwar@stonybrook.edu

Shrinath Deshpande

Computer-Aided Design and Innovation Lab,  
Department of Mechanical Engineering,  
Stony Brook University,  
Stony Brook, NY 11794-2300

Q. J. Ge

Computational Design Kinematics Lab,  
Department of Mechanical Engineering,  
Stony Brook University,  
Stony Brook, NY 11794-2300

*In this paper, we have presented a unified framework for generating planar four-bar motions for a combination of poses and practical geometric constraints and its implementation in MotionGen app for Apple's iOS and Google's Android platforms. The framework is based on a unified type- and dimensional-synthesis algorithm for planar four-bar linkages for the motion-generation problem. Simplicity, high-utility, and wide-spread adoption of planar four-bar linkages have made them one of the most studied topics in kinematics leading to development of algorithms and theories that deal with path, function, and motion generation problems. Yet to date, there have been no attempts to develop efficient computational algorithms amenable to real-time computation of both type and dimensions of planar four-bar mechanisms for a given motion. MotionGen solves this problem in an intuitive fashion while providing high-level, rich options to enforce practical constraints. It is done effectively by extracting the geometric constraints of a given motion to provide the best dyad types as well as dimensions of a total of up to six four-bar linkages. The unified framework also admits a plurality of practical geometric constraints, such as imposition of fixed and moving pivot and line locations along with mixed exact and approximate synthesis scenarios. [DOI: 10.1115/1.4035899]*

## 1 Introduction

Planar four-bar linkages are the most commonly used linkages in machines due to their simplicity, practicality, and performance characteristic that fit with a large number of path, function, and motion generation problems. In the last 50 years, numerous researchers have developed theories and algorithms for their synthesis and simulation leading to a large body of work which are now well-covered in text books by Sandor and Erdman [1], Uicker et al. [2], Norton [3], McCarthy and Soh [4], Hunt [5], Hartenberg and Denavit [6], Suh and Radcliffe [7], and several others.

Generation of mechanism design concepts is a critical step in the machine design process. This paper is concerned with the motion-generation problem, wherein a set of discrete poses (translation and orientation) are specified and the objective is to find both the type and dimensions of planar four-bar linkages. Here, *type* refers to the joint types and their pattern of interconnection. The current state-of-the-art in mechanism design follows a two-step approach, where machine designers typically use their past kinematic experience to first select a type and then use standard mathematical formulations to compute the dimensions of a linkage. While this two-step paradigm for mechanism design leads to better mechanism classification and enumeration [8,9], it makes type synthesis a very challenging task, even for those who have been well trained in mechanism science. Erdman and Sandor [10] summarized the importance and challenges of the type-synthesis problem. There have been several attempts to solve the combined problem of type synthesis and dimensional synthesis through the use of genetic algorithm [11,12], topology optimization [13,14], as well as a uniform polynomial system [15]. However, they have been carried out for very restricted applications with very limited number of mechanism types. More significantly, these approaches do not reduce the complexity of the type-synthesis problem. Researchers in artificial intelligence (AI) community have also sought with very limited success to bridge the gap between type and dimensional syntheses and developed what is known as *qualitative kinematics* [16] in the context of qualitative spatial reasoning.

Recently, we have shown that the ability to decompose a design problem into type and dimensional syntheses is actually data dependent and the type-synthesis problem may not be solved without engaging in dimensional synthesis simultaneously. This necessitates a data- or task-driven paradigm for simultaneous type and dimensional synthesis, see Ge et al. [17,18]. The key is to establish a computational approach for transforming the problem of *selecting* a mechanism type into that which is directly *computable* from the specified task, i.e., the quantitative information about a specified task drives the mechanism design process and is used to determine both the type and dimensions of a desired mechanism. In this paper, we present a unified framework, which not only incorporates the fixed positional constraints but also allows specifying practical geometric constraints, such as location of fixed and moving pivots of linkages at various locations or along certain lines, relaxing positional or geometric constraints to enable mixed exact and approximate synthesis without resorting to special cases. This framework is implemented in MotionGen.

MotionGen [19]<sup>2</sup> is an attempt to make the results of this work widely available to machine designers, practitioners, kinematicians, and students in the form of an accessible mobile app. The current pedagogical research literature indicates that the mobile technologies in education are serving as educational sandbox and removing the artificial boundaries between learning and playing while providing more time for hands-on activities that enhance student's cognition [20,21]. MotionGen is available for download for free for two industry-dominant platforms, viz., Apple iOS [22] and Google Android [23]. Mechanism synthesis systems coming from academia (KINSYN III [24], LINCAGES [25,26], Sphinxpc [27], Synthetica [28], Wu et al. [29], and Purwar and Gupta [30]) have mostly focused on dimensional synthesis. Although there are a few desktop software systems available for planar linkages that provide extensive simulation and analysis capabilities [31–35], none provides true synthesis capabilities that would enable users to engage in mechanism design innovation at a fundamental level. On the other hand, the MotionGen can *compute* both the type and dimensions of the linkages. Autodesk's Force Effect Motion [36] was one of the few mobile apps that provided simulation capabilities for *N*-bar linkages, however, sadly it is no longer available. More recently Turkkan and Su [37] presented a MATLAB tool for

<sup>1</sup>Corresponding author.

Manuscript received October 17, 2016; final manuscript received January 13, 2017; published online March 9, 2017. Assoc. Editor: Venkat Krovi.

<sup>2</sup><http://www.motiongen.io>

kinetostatic synthesis of compliant mechanisms, while Kinzel et al. [38] proposed a geometric constraint programming approach for mechanism synthesis in a host computer aided design environment. Lately, Disney Research, driven by a desire to physically animate their cartoon characters and build mechanically functional artifacts and robots for their entertainment parks, has invested in developing intuitive and efficient Linkage Editing software systems [39,40]. However, they have not made them available for public use. A detailed review of the state-of-the-art in computer-aided mechanism design software systems can be found in Chase et al. [41] and is summarized in Purwar et al. [42].

The rest of this paper is organized as follows: In Sec. 2, we review our overall approach for extraction of geometric constraints from a given motion and present the concept of planar kinematic mapping. Section 3 reviews a unified form of geometric constraints of dyads, while Sec. 4 presents how additional geometric constraints on poses and pivots can be unified as well. In Sec. 5, we show how various constraints can be solved for by employing a two-step process wherein first given constraints are algebraically fitted and then kinematic constraints are applied to extract the dyad type and dimensions. In Sec. 6, we present a few case studies illustrating the efficiency and efficacy of our approach.

## 2 Approach

MotionGen synthesizes planar four-bar linkages by computing appropriate planar RR, RP, and PR dyads and their dimensions for a given motion, where R refers to a revolute and P refers to a prismatic joint. When two such dyads are assembled, the coupler interpolates through the given poses either exactly or approximately while minimizing an algebraic fitting error. The algorithm employed in MotionGen extracts the geometric constraints (circular, fixed-line, or line-tangent-to-a-circle) implicit in the motion of an object and matches it with a corresponding mechanical dyad type. Given an arbitrary motion, MotionGen can compute the dyad types (RR, PR, and RP) that minimize the algebraic error of fitting the geometric constraints of these dyads with the motion. In the process of computing the types, the dimensions of the dyads are also computed. Due to the degree of polynomial system created in the solution, up to a total of six four-bar linkages can be computed for a given motion.

MotionGen also lets users simulate planar four-bar linkages by assembling the constraints of planar dyads on a grid- or image-overlaid screen. This constraint-based simulation approach mirrors the synthesis approach and allows users to input simple geometric features (circles and lines) for assembly and animation to verify the motion and make interactive changes to the trajectories.

Now, we review the details of this approach in so far as necessary to describe the algorithm behind MotionGen, see Ref. [17] for details. The mathematical machinery in MotionGen is based on use of planar quaternions for the representation of planar displacement, kinematic mapping, and a unified algebraic form of geometric constraints of dyads and other practical constraints written using homogeneous coordinates.

**2.1 Planar Kinematic Mapping.** A planar displacement consisting of a translation  $(d_1, d_2)$  and a rotation angle  $\phi$  from a moving frame  $M$  to a fixed frame  $F$  is represented by a planar quaternion  $\mathbf{Z} = (Z_1, Z_2, Z_3, Z_4)$  where (see Refs. [43] and [44] for details)

$$\begin{aligned} Z_1 &= \frac{1}{2} \left( d_1 \cos \frac{\phi}{2} + d_2 \sin \frac{\phi}{2} \right), & Z_2 &= \frac{1}{2} \left( -d_1 \sin \frac{\phi}{2} + d_2 \cos \frac{\phi}{2} \right) \\ Z_3 &= \sin \frac{\phi}{2}, & Z_4 &= \cos \frac{\phi}{2} \end{aligned} \quad (1)$$

The components  $(Z_1, Z_2, Z_3, Z_4)$  define a point in a projective three-space called the *image space* of planar displacements [44]. Then, a planar displacement represented as a homogeneous

transformation of point  $\mathbf{x} = (x_1, x_2, x_3)$  or line  $\mathbf{l} = (l_1, l_2, l_3)$  from  $M$  to  $F$  can be given by

$$\mathbf{X} = [H]\mathbf{x}, \quad [H] = \begin{bmatrix} Z_4^2 - Z_3^2 & -2Z_3Z_4 & 2(Z_1Z_3 + Z_2Z_4) \\ 2Z_3Z_4 & Z_4^2 - Z_3^2 & 2(Z_2Z_3 - Z_1Z_4) \\ 0 & 0 & Z_3^2 + Z_4^2 \end{bmatrix} \quad (2)$$

$$\mathbf{L} = [\overline{H}]\mathbf{l}, \quad [\overline{H}] = \begin{bmatrix} Z_4^2 - Z_3^2 & -2Z_3Z_4 & 0 \\ 2Z_3Z_4 & Z_4^2 - Z_3^2 & 0 \\ 2(Z_1Z_3 - Z_2Z_4) & 2(Z_2Z_3 + Z_1Z_4) & Z_3^2 + Z_4^2 \end{bmatrix} \quad (3)$$

where  $Z_3^2 + Z_4^2 = 1$ , and  $\mathbf{X} = (X_1, X_2, X_3)$  and  $\mathbf{L} = (L_1, L_2, L_3)$  are the corresponding point and line coordinates in  $F$ .

## 3 A Unified Form of Geometric Constraints of Dyads

Mechanical dyads of types RR, PR, and RP in planar four-bar linkages impose circle-, line-, or line-tangent-to-circle constraints on the end-effector, respectively. We disregard PP dyads due to their inability to effect a change in orientation. Using kinematic mapping, these geometric constraints can be written in a unifying algebraic form. Let  $\mathbf{a} = (a_1, a_2, a_0)$ , where  $a_0 \neq 0$ , denote the homogeneous coordinates of the center of a circle  $C$  in  $F$ . Then, a point with homogeneous coordinates  $\mathbf{X} = (X_1, X_2, X_3)$  lies on  $C$  if

$$2a_1X_1 + 2a_2X_2 + a_3X_3 = a_0 \left( \frac{X_1^2 + X_2^2}{X_3} \right) \quad (4)$$

The radius  $r$  of the circle is given by  $r^2 = (a_1/a_0)^2 + (a_2/a_0)^2 + a_3/a_0$ . When  $a_0 = 0$ , Eq. (4) becomes linear

$$L_1X_1 + L_2X_2 + L_3X_3 = 0 \quad (5)$$

which represents a line with homogeneous coordinates  $\mathbf{L} = (2a_1, 2a_2, a_3)$ . Thus, Eq. (4) is a unified representation for both a circle and a line, and therefore, could lead to a unified representation of the constraints of RR and PR dyads.

For an RP dyad, a line with homogeneous coordinates  $\mathbf{L} = (L_1, L_2, L_3)$  passes through a fixed point  $\mathbf{X} = (X_1, X_2, X_3)$ . In other words, they also satisfy Eq. (5).

Thus, we may conclude that all the three dyadal constraints can be represented by Eq. (4) and that when  $a_0 = 0$ , the dyad has at least one prismatic joint.

By substituting Eq. (2) into Eq. (4), we have shown in Ref. [45] that the constraint manifold of an RR dyad is the following quadratic surface in the image space:

$$\begin{aligned} p_1(Z_1^2 + Z_2^2) + p_2(Z_1Z_3 - Z_2Z_4) + p_3(Z_2Z_3 + Z_1Z_4) \\ + p_4(Z_1Z_3 + Z_2Z_4) + p_5(Z_2Z_3 - Z_1Z_4) + p_6Z_3Z_4 \\ + p_7(Z_3^2 - Z_4^2) + p_8(Z_3^2 + Z_4^2) = 0 \end{aligned} \quad (6)$$

where the eight coefficients  $p_i$  are not independent but must satisfy two quadratic conditions

$$p_1p_6 + p_2p_5 - p_3p_4 = 0, \quad 2p_1p_7 - p_2p_4 - p_3p_5 = 0 \quad (7)$$

This is because  $p_i$  are related to the geometric parameters of the dyad by

$$\begin{aligned} p_1 &= -a_0, & p_2 &= a_0x & p_3 &= a_0y, & p_4 &= a_1, & p_5 &= a_2 \\ p_6 &= -a_1y + a_2x, & p_7 &= -(a_1x + a_2y)/2 \\ p_8 &= (a_3 - a_0(x^2 + y^2))/4 \end{aligned} \quad (8)$$

where  $(a_0, a_1, a_2, a_3)$  are the homogeneous coordinates of the constraint circle expressed in fixed reference frame, and  $(x, y)$  are the

coordinates of the circle point expressed in moving reference frame. For a PR dyad, we have  $a_0=0$ , and therefore,  $p_1=p_2=p_3=0$ . Equations (6) and (7) are said to define the constraint manifold of RR and PR dyads.

By substituting Eq. (3) into Eq. (5), it is found that for RP dyad, the constraint manifold has the same form as Eqs. (6) and (7), however, we now have  $p_1=p_4=p_5=0$ . Thus, all the planar dyads can be represented in the same form by Eqs. (6) and (7), and we can determine the type of a planar dyad by looking at the zeros in the coefficients  $p_i$  (called signature of a dyad). This leads to a unified algorithm for simultaneous type and dimensional synthesis of planar dyads. In addition, this formulation eliminates the need for solving a large system of polynomial equations, which makes linkage synthesis problem challenging even for dimensional synthesis. In our approach, we first obtain the homogeneous coordinates  $p_i$ , determine the dyad type from the signature of coefficient array  $p_i$ , and then compute the dyad parameters using inverse relationships in Eq. (8).

#### 4 A Unified Form of Additional Practical Geometric Constraints

In this section, we show that apart from a set of positions, a plurality of practical geometric constraints can also be specified, which are all handled similarly in our unified framework without increasing the polynomial complexity. Although adding additional constraints may seem to shrink the design space for linkage synthesis, it expands intuitive horizon of mechanism designer. The additional constraints considered are specification of (1) additional pose constraint for mixed exact and approximate synthesis, (2) fixed- or moving-pivot locations at given points, and (3) specification of fixed- or moving-pivot locations on given lines. This framework derives its strength from the fact that any combinations of these constraints can be specified simultaneously to enable designers to realize their design goal. Thus, a problem may be specified as  $n$  positional or pivot constraints, some of which may be exact or approximate. Since, our algorithm computes dyads that solve for these constraints, any combination of two dyads may be assembled together to form many planar four-bar linkages.

**4.1 Pose Constraint for Mixed Exact and Approximate Positions.** For more than five pose constraints, in general, only an approximate solution may be obtained. However, up to five exact poses can still be specified to enable generation of planar four-bar linkages that can go through some poses exactly while approximating others. Pick-and-place operations fall under this category of problem, wherein the first and the last poses are exact constraints while in-between poses are to be synthesized only approximately. Specifying a fixed pose for such problems amounts to substituting for the displacement coordinates in Eq. (6), which provides an additional linear equation as follows:

$$\sum_{j=1}^8 A_{ij}p_j = 0 \quad (9)$$

where  $A_{ij}$  are known in terms of the planar quaternion coordinates. Together with the two quadratic constraints in Eq. (7) and the above linear constraint define the mixed exact- and approximate-synthesis problem, where up to five exact poses may be specified.

**4.2 Line Constraint for Pivots.** Line constraint for fixed pivots constrains the center point  $(X_c, Y_c)$  of an RR dyad to a line  $L_1X_c + L_2Y_c + L_3=0$ . Using inverse relationships in Eq. (8), we obtain a linear equation in  $p_i$  given by

$$-L_1p_4 - L_2p_5 + L_3p_1 = 0 \quad (10)$$

A similar constraint equation is obtained when the moving pivot of an RR dyad is constrained to a line  $(l_1, l_2, l_3)$  fixed in the moving frame given by

$$-l_1p_2 - l_2p_3 + l_3p_1 = 0 \quad (11)$$

Both of the above two constraints are in a form similar to Eq. (9) except that certain  $p_i$  are zero and the  $A_{ij}$  are in terms of the line coordinates. The two quadratic constraints in Eq. (7) and the above linear constraint define the problem where the fixed or moving pivots are to lie on a given line.

**4.3 Point Constraints for Pivots.** Specifying locations for fixed or moving pivots of the mechanism proves to be useful in practice as well. Let  $(X_c, Y_c)$  be one of these fixed-pivot locations. Each fixed-pivot location forms two linear equations in  $p_i$ , which using inverse kinematic relations for RR dyads can be given as

$$\begin{aligned} X_c p_1 + p_4 &= 0 \\ Y_c p_1 + p_5 &= 0 \end{aligned} \quad (12)$$

It is worth noting that all the types of dyads may not satisfy the imposed point constraints. This is due to fact that all the RP dyads have dyad coefficients  $p_1, p_4$ , and  $p_5$  zero, so they automatically satisfy Eq. (12) but do not necessarily have fixed pivot on specified location. This problem can be easily tackled by filtering out the extraneous solutions. Moving-pivot locations can also be provided in the same way as fixed-pivot locations. They too form two linear equations given by

$$\begin{aligned} x_m p_1 + p_2 &= 0 \\ y_m p_1 + p_3 &= 0 \end{aligned} \quad (13)$$

where  $(x_m, y_m)$  are the coordinates of moving-pivot location in moving reference frame. Once again, all the pivot location constraints are linear and in the same form as Eq. (9). The two quadratic constraints in Eq. (7) and the above two linear constraints define the problem where the fixed or moving pivots are located at a given point.

#### 5 Algebraic Fitting of Given Motion to the Geometric Constraints

We have seen that for motion-generation problems, the inputs are task poses and line and point constraints. These input constraints are linear equations in  $p_i$  of the form

$$\sum_{j=1}^8 A_{ij}p_j = 0 \quad (14)$$

where  $A_{ij}$  depends upon the type of  $i$ th input constraint, i.e., pose, line, or point constraint. Thus, given  $n$  pose or pivot constraints, we can write  $n$  linear equations in  $p_i$ . In matrix form, they are given by

$$\begin{aligned} [A] \begin{bmatrix} p_1 \\ p_2 \\ \vdots \\ p_8 \end{bmatrix} &= 0, \text{ where } [A] \\ &= \begin{bmatrix} A_{11} & A_{12} & A_{13} & A_{14} & \cdots & \cdots & \cdots & A_{18} \\ A_{21} & A_{22} & A_{23} & A_{24} & \cdots & \cdots & \cdots & A_{28} \\ \vdots & \vdots & \vdots & \vdots & \vdots & \vdots & \vdots & \vdots \\ A_{n1} & A_{n2} & A_{n3} & A_{n4} & \cdots & \cdots & \cdots & A_{n8} \end{bmatrix} \end{aligned} \quad (15)$$

This system of equations can be solved using least-square fitting via a matrix decomposition approach, such as singular value decomposition (SVD) [46]. As the matrix  $[A]^T[A]$  is  $8 \times 8$  and positive semidefinite, all the eigenvalues are non-negative and the eigenvector associated with the smallest of the eight eigenvalues is a "candidate" solution for  $\mathbf{p} = (p_1, p_2, \dots, p_8)$ .

Burmester [47] showed that a planar four-bar linkage can go through five poses ( $n=5$ ) exactly. However, in our formulation,

we need not distinguish between poses and other constraints—finite set of linkages are obtained nonetheless. The problem could be given as five task poses, four poses with a line constraint, three poses with a fixed point constraint or even two poses with a point and line constraint. When  $n=5$ , the system of equation is fully constrained as there are five dyad parameters to determine, and thus, the effective rank of the matrix  $[A]$  is five. In this case, the matrix  $[A]^T[A]$  has three zero eigenvalues and the corresponding eigenvectors,  $\mathbf{v}_\alpha$ ,  $\mathbf{v}_\beta$ , and  $\mathbf{v}_\gamma$ , define the basis for the null space. Let  $\alpha$ ,  $\beta$ , and  $\gamma$  denote three real parameters. Then, any vector in the null space is given by

$$\mathbf{p} = \alpha\mathbf{v}_\alpha + \beta\mathbf{v}_\beta + \gamma\mathbf{v}_\gamma \quad (16)$$

For vector  $\mathbf{p}$  to satisfy Eq. (7), we substitute Eq. (16) into Eq. (7) and obtain two homogeneous quadratic equations in  $(\alpha, \beta, \text{and } \gamma)$

$$\begin{aligned} K_{10}\alpha^2 + K_{11}\beta^2 + K_{12}\alpha\beta + K_{13}\alpha\gamma + K_{14}\beta\gamma + K_{15}\gamma^2 &= 0 \\ K_{20}\alpha^2 + K_{21}\beta^2 + K_{22}\alpha\beta + K_{23}\alpha\gamma + K_{24}\beta\gamma + K_{25}\gamma^2 &= 0 \end{aligned} \quad (17)$$

where  $K_{ij}$  are defined by components of the three eigenvectors, which can be obtained from using singular value decomposition of  $[A]$  [46].

Solving Eq. (17) and substituting in Eq. (16) would lead to the homogeneous coordinates of dyads. By investigating the patterns of zeros<sup>3</sup> in  $\mathbf{p} = (p_1, p_2, \dots, p_8)$ , one can also determine which of the three dyads, RR, PR, and RP, should be used for the given task. Thus, the aforementioned task analysis algorithm may yield up to four dyads from the solution of two quadratic equations in Eq. (7), two of which can be combined to form up to six four-bar linkages. Design parameters such as  $(x, y)$  and  $(a_0, a_1, a_2, a_3)$  can be obtained by inverting Eq. (8).

### 5.1 Null-Space Modification for Additional Constraints.

When  $n > 5$ , the system of equation is overconstrained; however, a least-square error solution may still be found using the SVD approach. In this case, if the pose and geometric constraints are given arbitrarily, only an approximate solution can be found—none of the  $n$  constraints may be satisfied exactly. This forms the basis for tolerance-based synthesis not only for given poses but also for other constraints. Fortunately, the aforementioned approach can still be used by picking three eigenvectors corresponding to three smallest eigenvalues and using Eqs. (16) and (17). This amounts to selecting the minimal null-subspace that allows us to compute the five dyad parameters uniquely. Interestingly, it is still possible to specify up to five additional constraints that can be satisfied exactly. We discuss this possibility next.

If an extra linear constraint on the pivot locations is given, then apart from the two quadratic conditions, now we have an additional linear equation which also needs to be satisfied exactly. This can be solved by selecting a four-dimensional subspace from the full eight-dimensional null-space of  $[A]$ . Then, the dyad vector  $\mathbf{p}$  has four eigenvectors corresponding to the four smallest eigenvalues. If  $\mathbf{v}_\alpha$ ,  $\mathbf{v}_\beta$ ,  $\mathbf{v}_\gamma$ , and  $\mathbf{v}_\mu$  denote four eigenvectors associated with those eigenvalues, then an arbitrary vector  $\mathbf{p}$  is given by

$$\mathbf{p} = \alpha\mathbf{v}_\alpha + \beta\mathbf{v}_\beta + \gamma\mathbf{v}_\gamma + \mu\mathbf{v}_\mu \quad (18)$$

To compute  $(\alpha, \beta, \gamma, \mu)$ , apart from the two constraints in Eq. (7), we add a line constraint for pivots, i.e.,

$$k_1\alpha + k_2\beta + k_3\gamma + k_4\mu = 0 \quad (19)$$

The above is obtained by substituting for  $\mathbf{p}$  in Eq. (10) or Eq. (11). Due to the linearity of the additional constraints, the polynomial complexity of the system to be solved does not change. Thus, the

<sup>3</sup>In numerical implementation, a component of normalized vector  $\mathbf{p}$  is assumed to be zero if its value is less than  $10^{-8}$ .

two quadratic conditions (7) and (19) still lead to a single quartic equation, which is solved to compute  $(\alpha, \beta, \gamma, \mu)$ .

If two extra linear constraints on the pivot locations are given, then we select a five-dimensional null-subspace so as to be able to satisfy additional conditions exactly. If the corresponding eigenvectors are denoted by  $\mathbf{v}_\alpha$ ,  $\mathbf{v}_\beta$ ,  $\mathbf{v}_\gamma$ ,  $\mathbf{v}_\mu$ , and  $\mathbf{v}_\eta$ , then a vector in the null space is given by

$$\mathbf{p} = \alpha\mathbf{v}_\alpha + \beta\mathbf{v}_\beta + \gamma\mathbf{v}_\gamma + \mu\mathbf{v}_\mu + \eta\mathbf{v}_\eta \quad (20)$$

We may use two linear equations of the form (19) to limit solutions. If these two equations represent two intersecting lines, then the intersection point can be seen as location of the fixed or moving pivots. In this case,  $(\alpha, \beta, \gamma, \mu, \nu)$  are solved from Eq. (7) and two linear equations of the form (19).

Extending this further, it can be seen that when the full null-space of the matrix  $[A]$  is utilized, a maximum of five additional constraints can be satisfied, which is consistent with the fact that for a dyad determined by five independent design parameters, only five constraints are needed.

The mixed exact- and approximate-pose synthesis problem is an example of the preceding cases. In such problems, the designer desires a few poses to be exact. Whenever a pose is set to be exact, its linear constraint of the form (9) becomes part of the exact conditions to be satisfied apart from the quadratic conditions. For example, for a pick-and-place motion, where only the first and last poses are critical and should be interpolated exactly, in between poses can be approximately satisfied. Thus, assuming a total of  $n > 5$  given poses, including first and the last one, the matrix  $[A]$  is of size  $(n-2) \times 8$  consisting of pose constraints corresponding to approximate poses, while the system of constraint consists of quadratic conditions (7) and two linear equations obtained by substituting  $\mathbf{p}$  from Eq. (20) in Eq. (9).

In short, this approach leads to a unified algorithm for both exact synthesis (when  $n=5$ ) and approximate synthesis (when  $n > 5$ ) of planar dyads that can handle joint type and dimensional synthesis simultaneously. Even in the case when  $n \neq 5$ , up to five additional constraints can be satisfied exactly. This framework can accept any number of poses, points, or lines constraints in union of each other to find a pool of dyads which in turn can be selected two at a time to form various linkages. Thus, for example, the designer could specify a rectangular frame for a planar linkage on the boundary of which pivots are to be located and the framework would enumerate all the dyad solutions which satisfy this constraint. Then, the designer can pick two preferred dyads. This equivalence between a positional and a geometrical constraint leads to a rich system of high-level abstraction and flexibility for the designer.

## 6 Case Studies

In this section, four case studies illustrating primary functions of MotionGen are presented. First three case studies present different ways of synthesizing four-bar mechanism based on functional requirements of various machines and are based on examples presented in Russel et al. [48]. The last case study shows how a film-advancing four-bar mechanism can be simulated and reverse-engineered.

**6.1 Moving a Stamping Tool Through Five Positions.** Five position synthesis problem may have four, two, or no solutions for dyads, so there can be up to six linkages that can interpolate through given positions. The MotionGen can also perform approximate synthesis for more than five positions and allows specifying a few of those poses as exact as well.

*Problem statement.* In this problem, stamping operation is to be performed on the parts moving on a conveyer belt. The objective is to synthesize a four bar that guides stamping tool through specified precision positions in desired order as shown in Fig. 1. Positions data are given in Table 1. Die can be changed at pose 1,

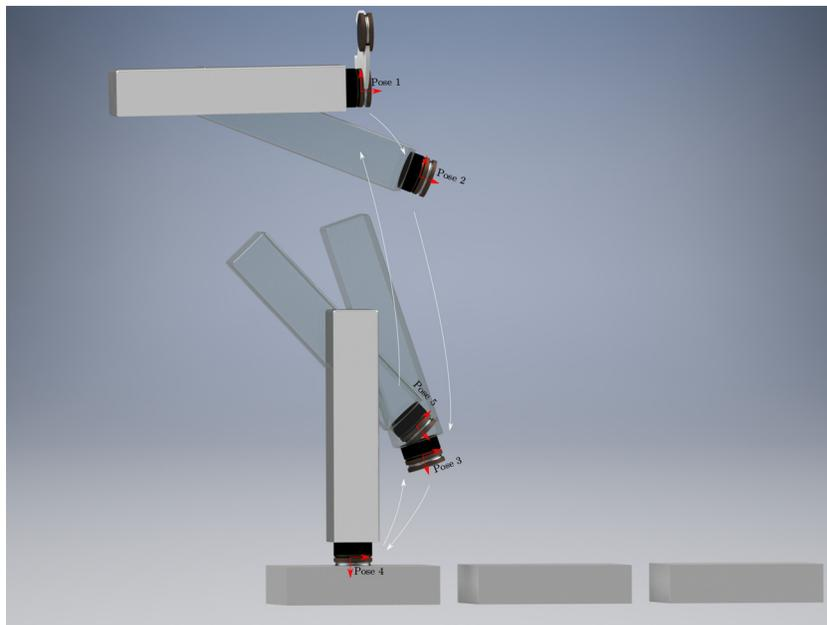


**Fig. 1** Five stamping poses; the stamping tool in first pose is almost horizontal, while in the fourth pose it is almost vertical

**Table 1** Poses for stamping tool

Poses	X	Y	$\phi$ (deg)
Pose 1	-1.081	2.132	1.0500
Pose 2	-0.484	1.268	338.42
Pose 3	-0.425	-1.436	287.26
Pose 4	-1.139	-2.438	271.23
Pose 5	-0.524	-1.158	316.10

while stamping is done at pose 4. Poses 1 and 4 are critical poses while remaining poses give a cyclic path that tool should follow, so they can be tweaked slightly if necessary.

As five positions are entered, all the possible dyads are computed. By clicking on dyads shown on the left side of screen in MotionGen, one can see the linkages and their respective coupler curves along with its motion animation. It is not trivial to find linkages free of circuit and branch defect; therefore, noncritical poses can be tweaked to find acceptable solutions. For this problem, four dyads of type RR are computed. Figure 2 shows a

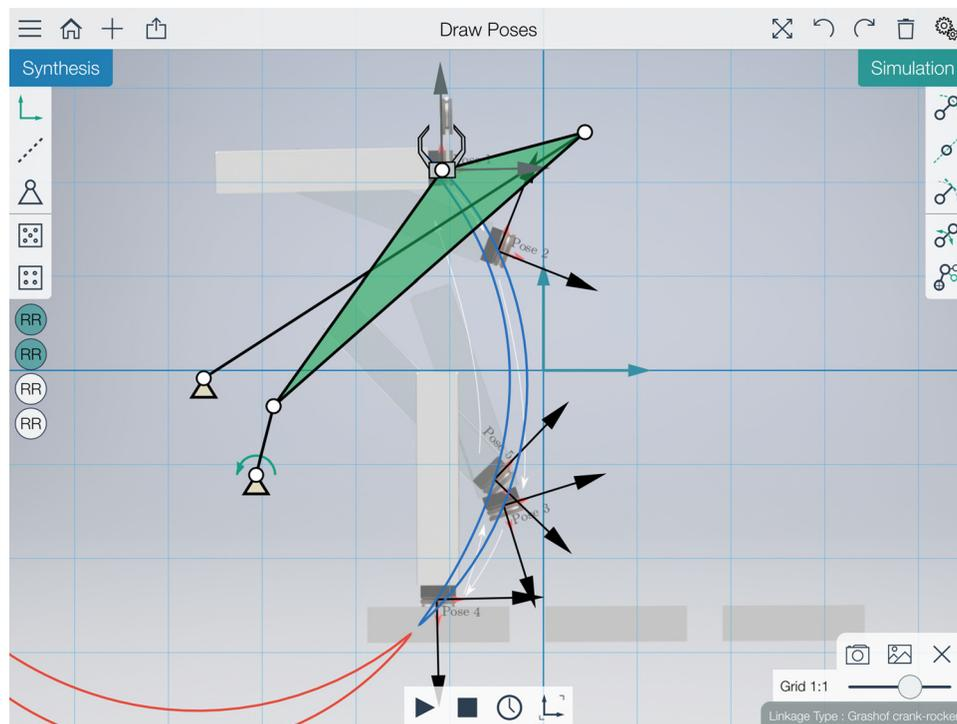


**Fig. 2** Stamping: Grashof crank-rocker solution; two curves shown are coupler curves in two different circuits

**Table 2 Stamping linkage joint data**

Point	X	Y
Fixed pivot 1	-3.0649	-1.1104
Moving pivot 1	-2.8790	-0.3815
Coupler point	-1.0806	2.1318
Moving pivot 2	0.4426	2.5354
Fixed pivot 2	-3.6238	-0.0837

Grashof RRRR linkage obtained by selecting first two dyads, while Table 2 contains joint information. All the joint-data information for linkage solutions in this paper are given in the fixed coordinate system when coupler is at the first pose, and the origin of the fixed coordinate frame in all the figures generated from the app is at the intersection of axes.

**6.2 Moving an Excavator Bucket Through Four Positions With Fixed-Line Constraint.** For four-position motion generation, we know that there are  $\infty^1$  number of planar four-bar linkages. Following approach outlined in Sec. 4, a finite number of solutions can be obtained by specifying: (1) a fixed-line constraint or (2) a moving-line constraint. This type of constraint keeps either fixed or moving pivots on a line specified.

*Problem Statement.* Synthesize a four-bar linkage which guides an excavator bucket in four precision positions as shown in Fig. 3. These poses are given in Table 3. Mechanism should be able to move the bucket in a cyclic way as shown in Fig. 3 to fulfill its function. Here, obtaining a Grashof mechanism is important, because bucket has to move from pose 3 to pose 1 without moving through pose 2. It is also desirable if all the fixed pivots are on a line that goes through poses 1 and 3, which will make it easy to mount it on the structure of vehicle.

When a fixed-line constraint is provided, all the possible dyad solutions are generated. The line can be tweaked to get different solutions. Table 4 gives the line constraint by listing its start point and orientation. As soon as this line is drawn on the screen, four RR, RR, RR, and RP dyads solutions are obtained. These dyads

**Table 3 Poses for the excavator bucket**

Poses	X	Y	$\phi$ (deg)
Pose 1	-2.1180	0.7620	269.59
Pose 2	-1.8250	-0.8310	296.62
Pose 3	0.7320	0.1410	358.67
Pose 4	0.9450	2.7390	279.98

**Table 4 Excavator: fixed-line constraint**

X	Y	$\phi$ (deg)
-1.6920	-0.2100	3.81

make up to six different linkages. By selecting two dyads shown on the left side of screen in MotionGen, one can see the assembled linkage, see Fig. 4. It can be seen that fixed pivots of the RR dyads are along the line which is desirable from mounting perspective. Table 5 contains joint data for the solution.

**6.3 Moving an Aircraft Landing Gear Through Three Positions With Two Fixed-Pivot Constraints.** Synthesizing a four-bar mechanism to guide the landing gear through three specified poses is selected to test three position synthesis problems with specified fixed-pivot constraints function of MotionGen.

*Problem Statement.* Synthesize a compact planar four-bar mechanism to guide the landing gear of an aircraft through the three precision positions as shown in Fig. 5, such that synthesized mechanism does not interfere with road at the landing position. The poses data for the problem are given in Table. 6.

*Choice of fixed pivots:* This problem has  $\infty^2$  solutions for RR dyads unless we specify either two moving or two fixed pivots of four bar. Choice of fixed pivots is motivated by ease of design, from structure and assembly point of view. For the first guess, fixed-pivot location chosen is near the fixed structure of aircraft so that hinges will be easy to mount. As soon as two fixed-pivot

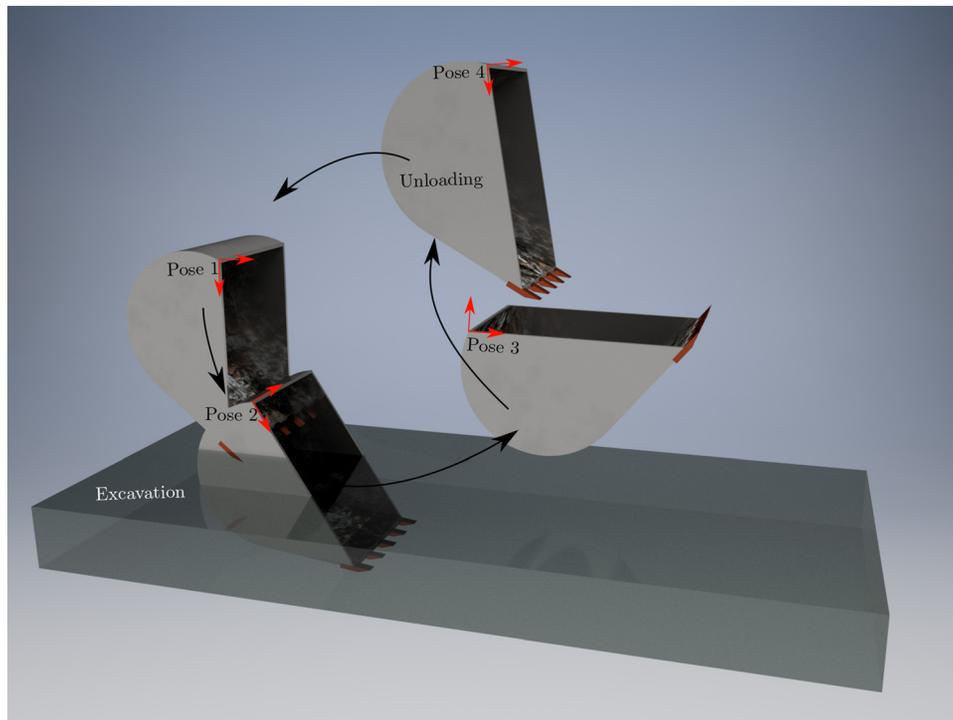


**Fig. 3 Excavator bucket motion through four positions**

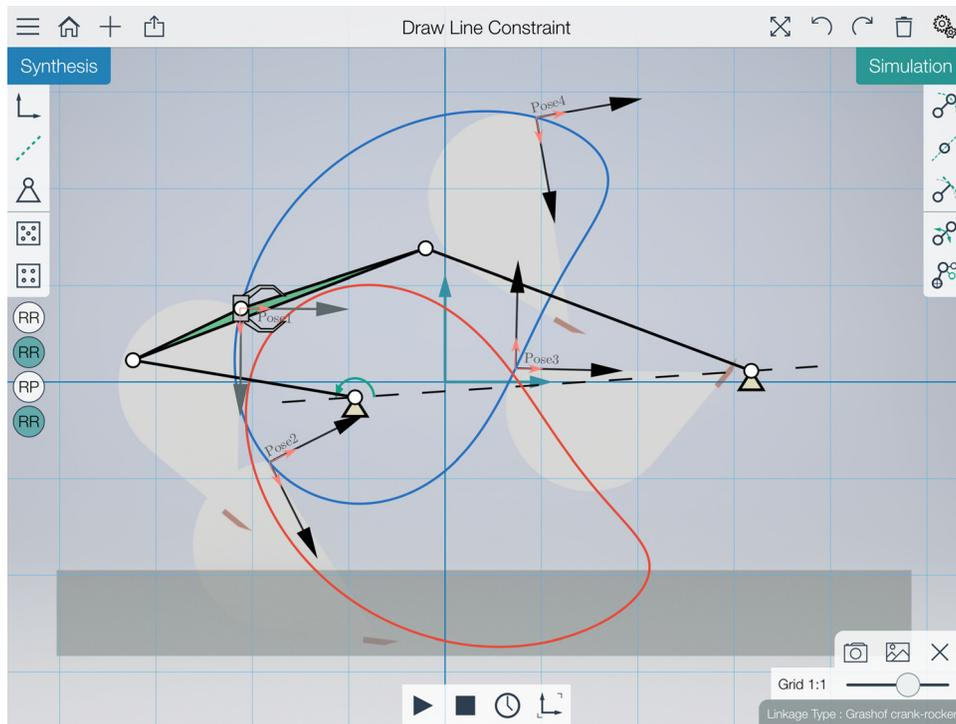


**Fig. 4 Excavator: Grashof crank-rocker linkage obtained by selecting two dyads**

**Table 5 Excavator linkage joint data: Grashof solution**

Point	X	Y
Fixed pivot 1	-0.9339	-0.1591
Moving pivot 1	-3.2388	0.2250
Coupler point	-2.1178	0.7620
Moving pivot 2	-0.2016	1.3827
Fixed pivot 2	3.1776	0.1150

**Table 6 Poses for landing gear**

Poses	X	Y	$\phi$ (deg)
Pose 1	0.258	1.658	333.69
Pose 2	0.205	0.957	11.500
Pose 3	-0.061	0.270	57.160

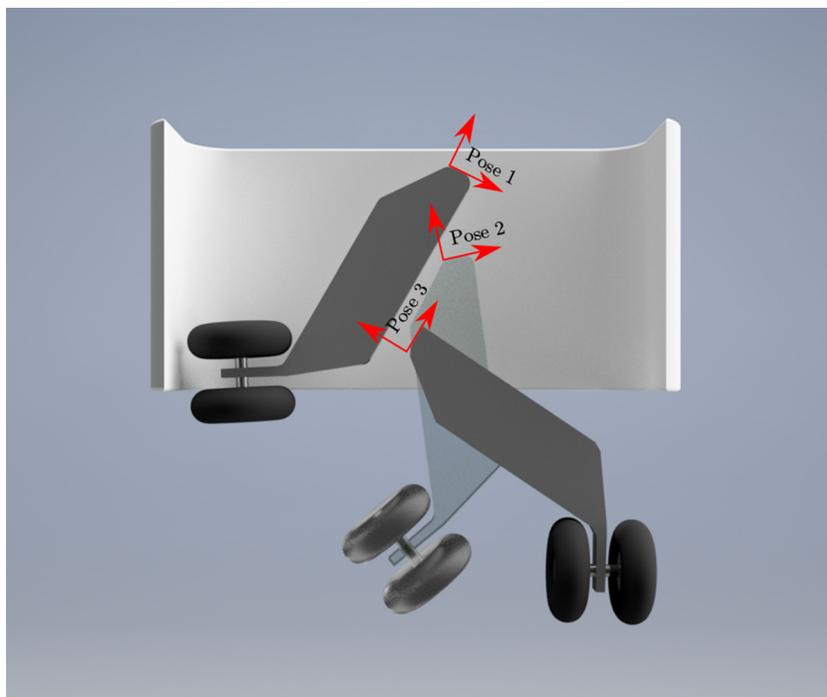


**Fig. 5 Poses for landing gear**

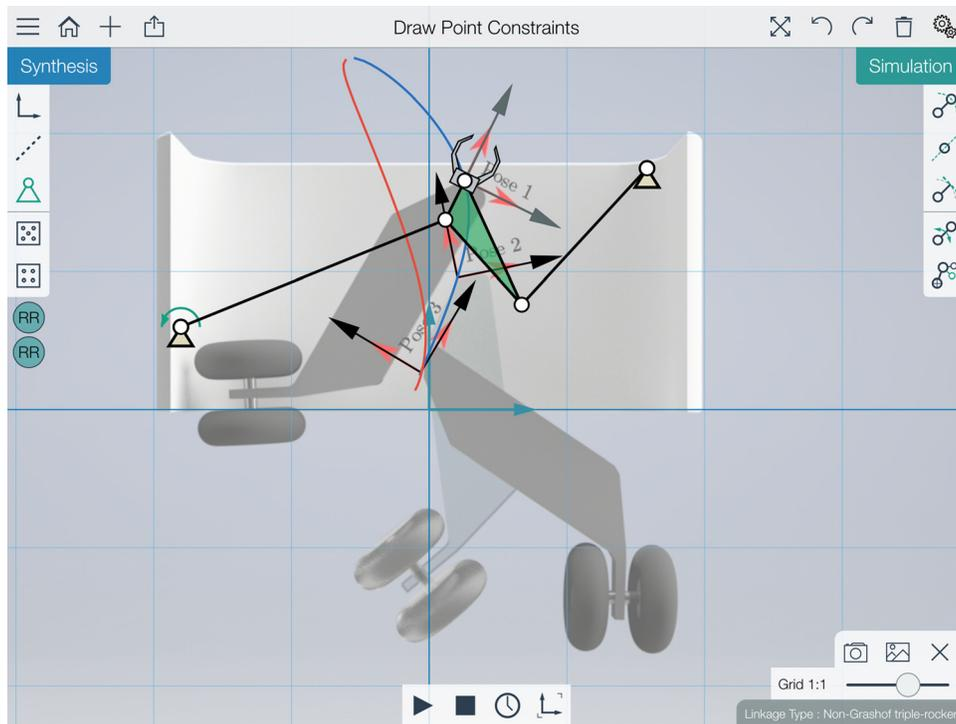


**Fig. 6 Landing gear: non-Grashof triple-rocker linkage**

**Table 7 Landing gear linkage joint data: non-Grashof solution**

Point	X	Y
Fixed pivot 1	-1.8031	0.5992
Moving pivot 1	0.1181	1.3752
Coupler end point	0.2581	1.6584
Moving pivot 2	0.6720	0.7609
Fixed pivot 2	1.5822	1.7479

locations are provided, MotionGen synthesizes all the possible dyads. The mechanism shown in Fig. 6 has fixed pivots mounted on the structure. The mechanism has small sized links, which helps in weight reduction and mechanism does not interfere with road, however, it is a non-Grashof type four bar. This solution can be useful if Grashof mechanism is not a necessary criterion. Table 7 contains joint data for the selected mechanism.

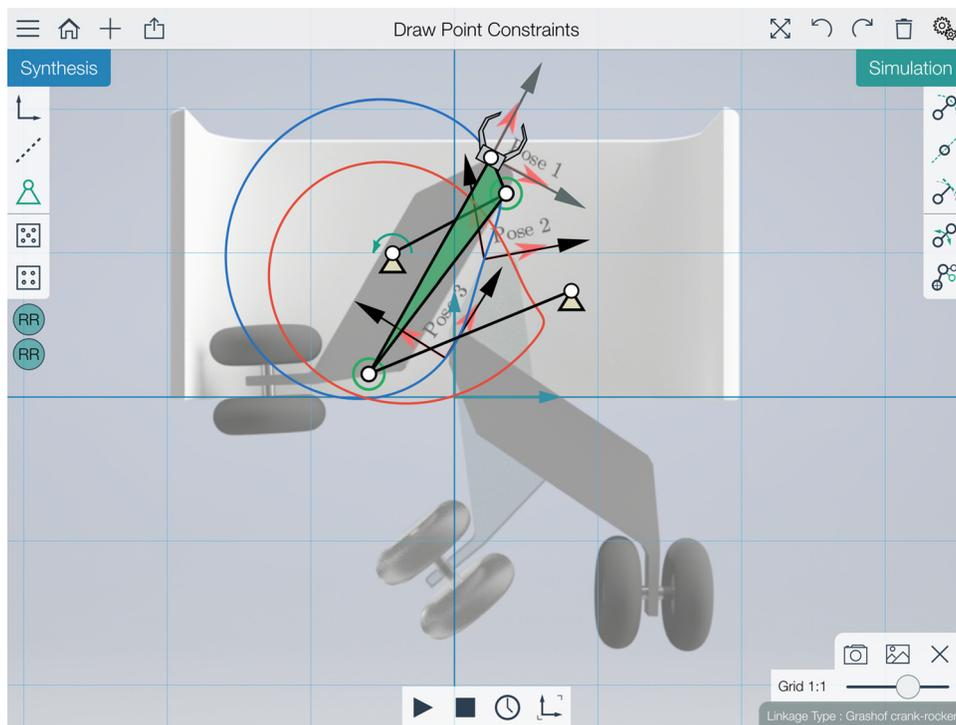


**Fig. 7 Landing gear: Grashof crank-rocker linkage**



**Table 8 Landing gear linkage joint data: Grashof solution**

Point	X	Y
Fixed pivot 1	-0.4304	0.9989
Moving pivot 1	0.3603	1.4139
Coupler end point	0.2544	1.6638
Moving pivot 2	-0.5959	0.1603
Fixed pivot 2	0.8145	0.7390

Another strategy is to specify moving pivots to generate more solutions. Figure 7 shows a Grashof linkage obtained by using moving pivots, although links are bigger in size compared to the non-Grashof solution in Fig. 6. Table 8 contains the joint data for the linkage.

#### 6.4 Simulation and Reverse-Engineering of a Film-Advancing Mechanism.

Norton [3] presented an interesting planar four-bar film-advancing mechanism, which is shown in Fig. 8.

Accompanying the figure in the text is a description of how the mechanism works by pulling the film down through its perforations on the side. The description highlights the importance of engaging the coupler-hook into perforations almost horizontally, a vertically downward movement of the film and then at the lowest point, an almost horizontal retraction to avoid jamming. MotionGen allows importing a picture of a mechanism and drawing on top of it to appreciate how the linkage really works. In this case, two RR dyads are drawn over the image by approximately matching the fixed pivots, moving pivots, and the coupler point. Once it is drawn, coupler curves are computed and displayed on the screen as shown in Fig. 8 and the mechanism can be animated.

If a practical constraint arises that mechanism can only be allowed to mount along a specified line, then mechanism can be reverse-engineered using the pose capture tool in MotionGen. While mechanism is animated, four positions are captured. These four positions are then fed to synthesis algorithm along with specified line constraint. Resulted reverse-engineered mechanism is shown in Fig. 9.

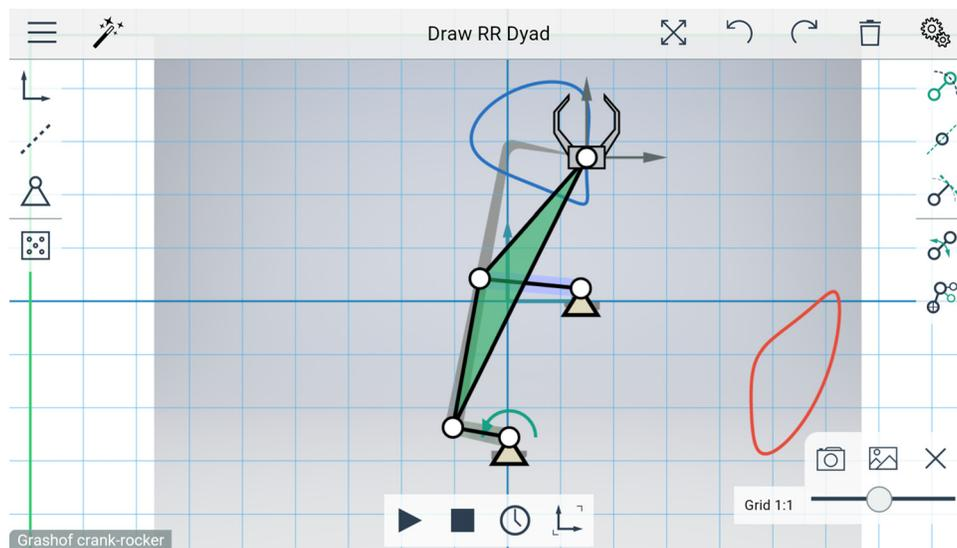


**Fig. 8 Simulation of planar four-bar film-advancing mechanism in Motiongen**

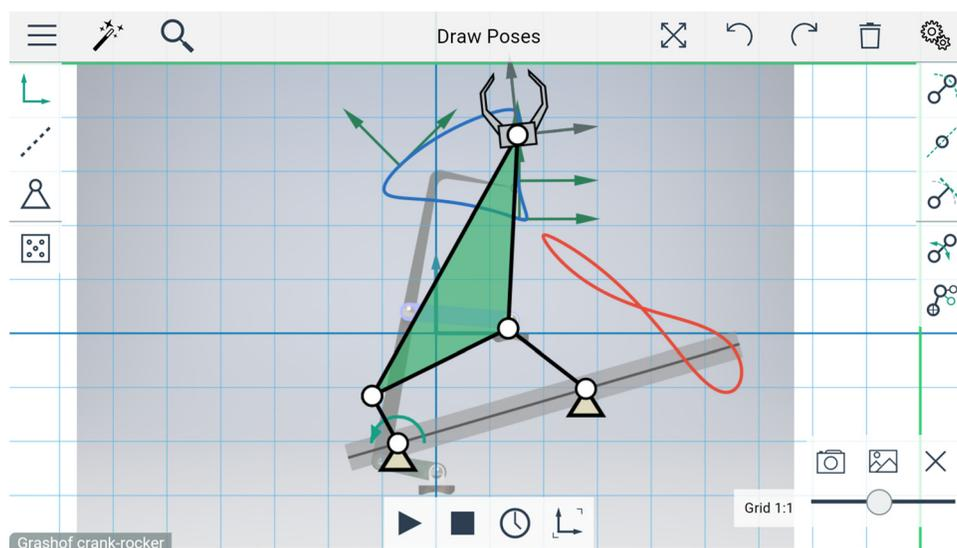


**Fig. 9 Reverse-engineered four-bar film-advancing mechanism satisfying a practical line constraint in MotionGen**

## 7 Conclusion

This paper presented a unified framework for synthesizing planar four-bar linkage type and dimensions under various pose and pivot constraints. The algorithm developed admits an arbitrary number of such constraints. This algorithm is implemented in a universal mobile app called MotionGen, which performs real-time computation of planar four-bar linkages for a given motion and other practical constraints. Instead of taking a black-box approach for solving the problem, the app provides multiple pathways to innovation by facilitating a dialog with the designer. MotionGen has been tested on various contemporary Apple and Android devices, and no significant difference in performance was found. It was also found that there is no cognizable lag in real-time computation for any kind of input or complexity. A number of case studies demonstrating the efficacy of the app were presented.

## Acknowledgment

This work was supported by the National Science Foundation under Grant No. CMMI-1563413. We also acknowledge the support from a TALENT grant [49] from Stony Brook University's Teaching, Learning and Technology (TLT) Program and a SUNY Innovative Instruction Technology (IITG) award [50] for the development of MotionGen. Anshul Lodha assisted with creating the computer aided design renderings in this paper. We are also indebted to the reviewers of this paper whose comments have made this a better work.

## References

- [1] Sandor, G. N., and Erdman, A. G., 1997, *Advanced Mechanism Design: Analysis and Synthesis*, Vol. 2, Prentice Hall, Englewood Cliffs, NJ.
- [2] Uicker, J. J., Pennock, G. R., and Shigley, J. E., 2011, *Theory of Machines and Mechanisms*, 4th ed., Oxford University Press, New York.
- [3] Norton, R., 2011, *Design of Machinery: An Introduction to the Synthesis and Analysis of Mechanisms and Machines*, 5th ed., McGraw Hill, New York.
- [4] McCarthy, J. M., and Soh, G. S., 2010, *Geometric Design of Linkages*, Vol. 11, Springer, New York.
- [5] Hunt, K., 1978, *Kinematic Geometry of Mechanisms*, Clarendon Press, Oxford, UK.
- [6] Hartenberg, R. S., and Denavit, J., 1964, *Kinematic Synthesis of Linkages*, McGraw-Hill, New York.
- [7] Suh, C. H., and Radcliffe, C. W., 1978, *Kinematics and Mechanism Design*, Wiley, New York.
- [8] Tsai, L., 2001, *Mechanism Design: Enumeration of Kinematic Structures According to Function*, CRC Press LLC, Boca Raton, FL.
- [9] Mruthunjaya, T., 2003, "Kinematic Structure of Mechanisms Revisited," *Mech. Mach. Theory*, **38**(4), pp. 279–320.
- [10] Erdman, A. G., and Sandor, G. N., 1991, *Mechanism Design: Analysis and Synthesis*, Vol. 1, 2nd ed., Prentice Hall, Englewood Cliffs, NJ.
- [11] Eberhard, P., Gausele, T., and Sedlaczek, K., 2009, "Topology Optimized Synthesis of Planar Kinematic Rigid Body Mechanisms," *Advanced Design of Mechanical Systems: From Analysis to Optimization*, J. A. C. Ambrósio and P. Eberhard, eds., Springer, Vienna, Austria, pp. 287–302.
- [12] Fang, W., 1994, "Simultaneous Type and Dimensional Synthesis of Mechanisms by Genetic Algorithms-DE," *Mech. Synth. Anal.*, **70**, pp. 35–41.
- [13] Frecker, M. I., Ananthasuresh, G. K., Nishiwaki, S., Kikuchi, N., and Kota, S., 1997, "Topological Synthesis of Compliant Mechanisms Using Multi-Criteria Optimization," *ASME J. Mech. Des.*, **119**(2), pp. 238–245.
- [14] Saxena, A., and Ananthasuresh, G. K., 2003, "A Computational Approach to the Number of Synthesis of Linkages," *ASME J. Mech. Des.*, **125**(1), pp. 110–118.
- [15] Hayes, M., and Zsombor-Murray, P., 2004, "Towards Integrated Type and Dimensional Synthesis of Mechanisms for Rigid Body Guidance," *CSME Forum*, London, ON, June 1–4, pp. 53–61.
- [16] Faltings, B., 1990, "Qualitative Kinematics in Mechanisms," *Artif. Intell.*, **44**(1–2), pp. 89–119.
- [17] Ge, Q. J., Purwar, A., Zhao, P., and Deshpande, S., 2016, "A Task Driven Approach to Unified Synthesis of Planar Four-Bar Linkages Using Algebraic Fitting of a Pencil of G-Manifolds," *ASME Paper No. DETC2013-12977*.
- [18] Ge, Q. J., Zhao, P., Purwar, A., and Li, X., 2012, "A Novel Approach to Algebraic Fitting of a Pencil of Quadrics for Planar 4R Motion Synthesis," *ASME J. Comput. Inf. Sci. Eng.*, **12**(4), p. 041003.
- [19] Purwar, A., 2016, "MotionGen's Support Site," Stony Brook University, Stony Brook, NY, accessed Feb. 2, 2017, <http://www.motiongen.io>
- [20] Keengwe, J., and Bhargava, M., 2013, "Mobile Learning and Integration of Mobile Technologies in Education," *Educ. Inf. Technol.*, **19**(4), pp. 737–746.
- [21] West, D. M., 2013, "Mobile Learning: Transforming Education, Engaging Students, and Improving Outcomes," The Brookings Institution, Washington, DC, accessed Jan. 25, 2016, <http://www.brookings.edu/research/papers/2013/09/17-mobile-learning-education-engaging-students-west>
- [22] Purwar, A., 2016, "MotionGen for iOS," Stony Brook University, Stony Brook, NY, accessed Feb. 2, 2017, <https://itunes.apple.com/us/app/motiongen/id1065657088?ls=1&mt=8>
- [23] Purwar, A., 2016, "MotionGen for Android," Stony Brook University, Stony Brook, NY, accessed Feb. 2, 2017, <https://play.google.com/store/apps/details?id=com.stonybrookuniversity.motiongen&hl=en>
- [24] Rubel, A. J., and Kaufman, R. E., 1977, "Kinsyn III: A New Human-Engineered System for Interactive Computer-Aided Design of Planar Linkages," *ASME J. Eng. Ind.*, **99**(2), pp. 440–448.
- [25] Erdman, A., and Gustafson, J., 1981, "LINCAGES: Linkage Interactive Computer Analysis and Graphically Enhanced Synthesis Package," *ASME Paper No. 77-DET-5*.
- [26] Erdman, A. G., and Riley, D., 1981, "Computer-Aided Linkage Design Using the Linkages Package," *ASME Paper No. 81-DET-121*.
- [27] Ruth, D., and McCarthy, J., 1997, "Sphinxpc: An Implementation of Four Position Synthesis for Planar and Spherical 4R Linkages," *ASME Paper No. DETC97/DAC-3860*.
- [28] Su, H.-J., Collins, C., and McCarthy, J., 2002, "An Extensible Java Applet for Spatial Linkage Synthesis," *ASME Paper No. DETC2002/MECH-34371*.
- [29] Wu, J., Purwar, A., and Ge, Q. J., 2010, "Interactive Dimensional Synthesis and Motion Design of Planar 6R Single-Loop Closed Chains Via Constraint Manifold Modification," *ASME J. Mech. Rob.*, **2**(3), p. 31012.
- [30] Purwar, A., and Gupta, A., "Visual Synthesis of RRR- and RPR-Legged Planar Parallel Manipulators Using Constraint Manifold Geometry," *ASME Paper No. DETC2011-48830*.
- [31] Design Simulation Technologies, 2017, "Working Model 2D," Design Simulation Technologies, Canton, MI, accessed Feb. 2, 2017, <http://www.design-simulation.com/wm2d/>
- [32] Artas-Engineering, 2017, "SAM (Synthesis and Analysis of Mechanisms)," Artas-Engineering Software, Nuenen, The Netherlands, accessed Feb. 2, 2017, <http://www.artas.nl/en>
- [33] Norton Associates Engineering, 2017, "Linkages," Norton Associates LLC, Naples, FL, accessed Feb. 2, 2017, <http://www.designofmachinery.com/Linkage/>
- [34] KCP Technologies, 2017, "The Geometer's Sketchpad," KCP Technologies Limited, Chennai, India, accessed Feb. 2, 2017, <http://www.dynamicgeometry.com>
- [35] International GeoGebra Institute, 2017, "Geogebra," International GeoGebra Institute, Germany, accessed Feb. 2, 2017, <http://www.geogebra.org/cms/>
- [36] Autodesk, 2017, "ForceEffectMotion," Autodesk, San Rafael, CA, accessed Feb. 2, 2017, <http://www.autodesk.com/mobile-apps>
- [37] Turkkkan, O. A., and Su, H.-J., 2015, "A Software for Kinetostatic Synthesis of Compliant Mechanisms," *ASME Paper No. DETC2015-47578*.
- [38] Kinzel, E. C., Schmiedeler, J. P., and Pennock, G. R., 2006, "Kinematic Synthesis for Finitely Separated Positions Using Geometric Constraint Programming," *ASME J. Mech. Des.*, **128**(5), pp. 1070–1079.
- [39] Moritz, B., Stelian, C., and Bernhard, T., 2015, "LinkEdit: Interactive Linkage Editing Using Symbolic Kinematics," *ACM Trans. Graphics*, **34**(4), pp. 1–8.
- [40] Bernhard, T., Stelian, C., Damien, G., Vittorio, M., Eitan, G., and Markus, G., 2014, "Computational Design of Linkage-Based Characters," *ACM Trans. Graphics*, **33**(4), pp. 1–9.
- [41] Chase, T., Kinzel, G., and Erdman, A., 2013, "Computer Aided Mechanism Synthesis: A Historical Perspective," *Advances in Mechanisms, Robotics and Design Education and Research*, Vol. 14, Springer International Publishing, Cham, Switzerland, pp. 17–33.
- [42] Purwar, A., Toravi, A., and Ge, Q. J., 2014, "4MDS: A Geometric Constraint Based Motion Design Software for Synthesis and Simulation of Planar Four-Bar Linkages," *ASME Paper No. DETC2014-35235*.
- [43] McCarthy, J. M., 1990, *Introduction to Theoretical Kinematics*, The MIT Press, Cambridge, MA.
- [44] Ravani, B., and Roth, B., 1983, "Motion Synthesis Using Kinematic Mappings," *ASME J. Mech. Transm. Autom. Des.*, **105**(3), pp. 460–467.
- [45] Ge, Q. J., Zhao, P., and Purwar, A., 2013, "A Task Driven Approach to Unified Synthesis of Planar Four-Bar Linkages Using Algebraic Fitting of a Pencil of G-Manifolds," *ASME Paper No. DETC2013-12977*.
- [46] Golub, G., and Van Loan, C., 1996, *Matrix Computations*, Johns Hopkins University Press, Baltimore, MD.
- [47] Burmester, L., 1886, *Lehrbuch der Kinematik*, Verlag Von Arthur Felix, Leipzig, Germany.
- [48] Russell, K., Shen, Q., and Sodhi, R. S., 2014, *Mechanism Design: Visual and Programmable Approaches*, CRC Press, Boca Raton, FL.
- [49] Purwar, A., and Ge, Q. J., 2012, "TALENT Grant: Design and Development of an Innovative Machine Design App for Engineers and Others, Teaching, Learning, and Technology Center," Stony Brook University, Stony Brook, NY, accessed Feb. 2, 2017, <http://facultycenter.stonybrook.edu/pages/2012-grant-recipients>
- [50] Purwar, A., Ge, Q. J., and Aceves, P., 2013, "Freshman Design Innovation: SUNY Innovative Instruction Technology Grant (IITG)," State University of New York (SUNY), accessed Feb. 2, 2017, <http://commons.suny.edu/iitg/freshman-design-innovation/>